# Synthesis, characterization and catalytic reactivity of ruthenium nanoparticles stabilized by chiral N-donor ligands

**Susanna Jansat,[ab] David Picurelli,[a] Katrin Pelzer,[b] Karine Philippot,*[b] Montserrat Gómez,*[a] Guillermo Muller,[a] Pierre Lecante[c] and Bruno Chaudret*[b]**

***Received (in Montpellier, France) 4th July 2005, Accepted 15th November 2005***
***First published as an Advance Article on the web 7th December 2005***
**DOI: 10.1039/b509378c**



The decomposition of the organometallic precursor [Ru(cod)(cot)] (cod = 1,5-cyclooctadiene; cot = 1,3,5-cyclooctatriene) under mild conditions (room temperature, 3 bars $H_2$) and in the presence of optically pure ligands, **L***, namely (*R*)-2-aminobutanol **1**, amino(oxazolines) (**2**, **3**), hydroxy(oxazoline) (**4**) and bis(oxazolines) (**5–8**), leads to stable ruthenium nanoparticles exhibiting a mean diameter between 1.6–2.5 nm. These nanoparticles can be isolated and re-dispersed. They display different mean sizes, shapes and dispersions depending on the stabilizer nature. These new colloids (**Ru1**–**Ru18**) have been characterized by both solid state and molecular chemistry techniques, including TEM/HRTEM, WAXS, elemental analysis, and IR and NMR spectroscopy. To further characterize the surface state of these particles, their catalytic behaviour has been examined in the reduction of organic prochiral unsaturated substrates. Although the asymmetric induction obtained is modest, it reveals the influence of the asymmetric ligand coordinated at the surface of the particles.

## Introduction

The synthesis of well-defined metal nanoparticles has experienced tremendous development over the past few years, primarily due to their physical properties and their potential for applications in the field of micro/nanoelectronics.[1] Metal nanoparticles have also attracted interest because of their potential in catalysis.[2] As such nanoparticles have proven to be efficient and selective catalysts for reactions also catalyzed by molecular complexes, such as olefin hydrogenation or C–C coupling reactions,[3] but moreover for reactions which are not, or are poorly catalyzed by molecular species, such as aromatic hydrocarbon hydrogenation.[4] Unambiguous distinction between colloidal and true homogeneous catalysis is, however, often very difficult to make.[5]

During the last few years, we have studied the synthesis of metal nanoparticles using an organometallic approach.[6] This methodology has led to nearly monodisperse particles of very small size that display remarkable surface coordination chemistry. The use of spectroscopic techniques (IR, NMR in solution or in the solid state) has permitted the study of the coordination chemistry of amines at the surface of ruthenium nanoparticles, as well as their dynamic behaviour in solution.[7,8] Furthermore, such studies have evidenced the presence of surface hydrides on these same particles.[8] Another approach aimed at characterizing the presence of surface ligands focuses on the reactivity of the resulting nanoparticles, the best example being the selectivity often found in catalytic processes. Despite impressive progress in asymmetric catalysis, however, only a few colloidal systems have been shown to display specific behaviour. The most relevant systems involve Pt or Pd nanoparticles stabilized by cinchonidine, in the hydrogenation of pyruvate derivatives.[9]

We are therefore interested in metal nanoparticle reactivity, not only with the aim of identifying reactions which are not catalyzed by molecular complexes,[10] but also with the goal of characterizing those differences present in well-known reactions catalyzed by either molecular complexes or metal nanoparticles. In this respect, we have recently reported the use of palladium species stabilized by a chiral diphosphite for asymmetric allylic alkylation, and found that the use of nanoparticles leads to slower catalysts but displaying an important discrimination between the two enantiomers of racemic substrates.[11]

In the present study, we examine another well-known process catalyzed by molecular complexes, namely, asymmetric reduction of unsaturated substrates using dihydrogen or isopropanol in a basic medium as a hydrogen source. Ru nanoparticles were synthesized using nitrogen donor ligands such as β-amino alcohols (**1**) and chiral oxazolines (**2–8**), easily prepared from commercially available amino acids and nitrile or carboxylic acid derivatives (Fig. 1). A comparative catalytic study between colloidal and conventional molecular systems is also described.

The coordination chemistry of these chiral ligands, as well as their applications in several enantioselective catalytic processes, has been previously studied: specifically, the reduction of unsaturated substrates (Ru, Rh, Ir),[12] allylic substitutions (Pd)[13] and olefin epoxidations (Mo).[14] β-Amino alcohols,

[a] *Departament de Química Inorgànica, Universitat de Barcelona, Martí i Franquès 1-11, 08028 Barcelona, Spain E-mail: gomez@chimie.ups-tlse.fr*
[b] *Laboratoire de Chimie de Coordination du CNRS, 205, route de Narbonne, 31077 Toulouse Cédex 04, France. E-mail: chaudret@lcc-toulouse.fr. E-mail: phil@lcc-toulouse.fr*
[c] *Centre d'Elaboration des Matériaux et d'Etudes Structurales du CNRS, 29, rue Jeanne Marvig, BP 4347, 31055 Toulouse Cédex 04, France*

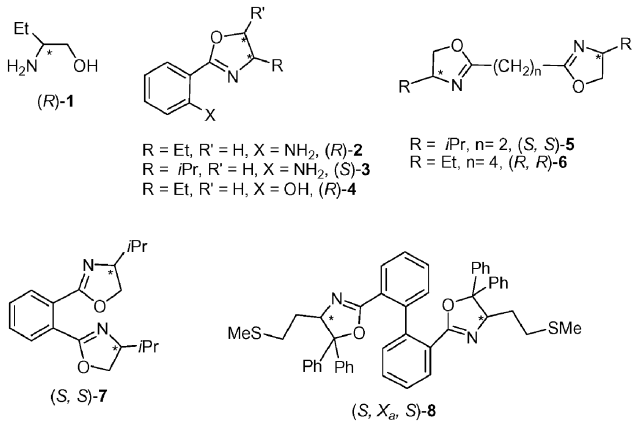


**Fig. 1** Chiral N-donor ligands: β-amino alcohol **1**, mono(oxazolines) **2–4**, and bis(oxazolines) **5–8**.

previously shown to be excellent chiral auxiliaries in Ru-catalyzed asymmetric hydrogen transfer processes,[15] were also examined. In this paper, we present the synthesis of new Ru nanoparticles, stabilized by both chiral β-amino alcohols and oxazolines, and their catalytic behaviour in the reduction of unsaturated substrates.

## Results and discussion

### Syntheses of ligands and stabilized nanoparticles

Four types of N-donor ligands (**1–8**) were used as stabilizers for the synthesis of Ru nanoparticles (**Ru1–Ru8**): β-amino alcohol (**1**), amino(oxazolines) (**2**, **3**), hydroxy(oxazoline) (**4**) and bis(oxazolines) (**5–8**) (Fig. 1). The oxazoline derivatives were synthesized following our previously described procedures,[12b,13] and obtained in a diastereomerically pure form, with the exception of **8**, which was separated as a mixture of two diastereomers due to its axial chirality.[13b] Phenyl-mono (oxazolines), **2–4**, contain alcohols or amines as functional groups in an *ortho*-position with respect to the heterocycle, capable of interacting with the nanoparticle surfaces.

Ruthenium colloids (**Ru1–Ru8**) were prepared following our previously reported procedure, but using the chiral ligands described above as stabilizers (Scheme 1).[7] In a typical experiment, the precursor [Ru(cod)(cot)][16] is dissolved at 193 K in a THF or THF–methanol solution containing 0.2 equivalents of the appropriate ligand, **L***, in a Fischer–Porter bottle (Scheme 1).

The resulting yellow solution is then exposed to a dihydrogen atmosphere (3 bar), allowed to warm to room temperature and stirred vigorously for 24 hours. Ligand stability was tested under the same conditions and no imine bond reduction was observed. The colloids obtained (**Ru1–Ru8**) were purified by precipitation upon the addition of pentane, followed by filtration and drying under reduced pressure, giving rise to a dark brown powder consisting of nanoparticles which could then be re-dispersed in THF or isopropanol. In all cases, the particles were found to be stable over time, and did not show any sign of decomposition under an argon atmosphere. The average yield of these syntheses after work-up was approximately 40%, based on ruthenium.

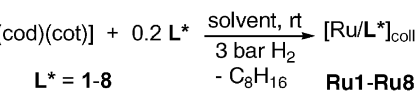


**Scheme 1** Synthesis of Ru colloids **Ru1–Ru8** stabilized by the corresponding ligands, **1–8**.

### Characterization of the nanoparticles

The sizes of the nanoparticles were determined by TEM (transmission electron microscopy) and their structures by WAXS (wide angle X-ray scattering), and in selected cases by HRTEM (high resolution transmission electron microscopy). In all instances, well-crystallized *hcp* nanoparticles of small size and narrow size distribution were obtained.

By using (*R*)-2-aminobutanol, (*R*)-**1**, nearly spherical monodisperse nanoparticles of isotropic shape and a mean size near 2.5 nm, were obtained (**Ru1**). These particles exhibited a strong tendency to self-assemble, as shown in Fig. 2. The coherence length measured on the WAXS spectrum was shorter than the size measured by TEM, a finding consistent with a lack of crystalline order throughout the nanoparticles (Fig. 3).

When amino(oxazolines) were used, particle sizes remained near 2.5 nm (**Ru2**, **Ru3**). These particles were well separated but showed a tendency to agglomerate on the microscopy grid (Fig. 4). In addition they also displayed a slightly anisotropic shape, which is more visible in **Ru3**. This, or a lack of crystallinity, may account for the shortening of coherence length, as measured by WAXS, in **Ru3** (Fig. 5).

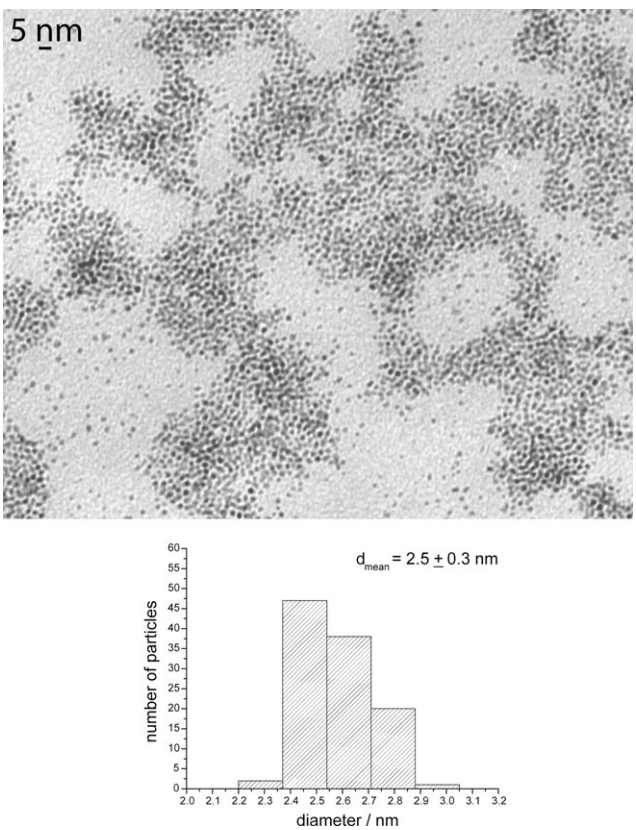


**Fig. 2** TEM micrograph and size histogram of **Ru1**.

 

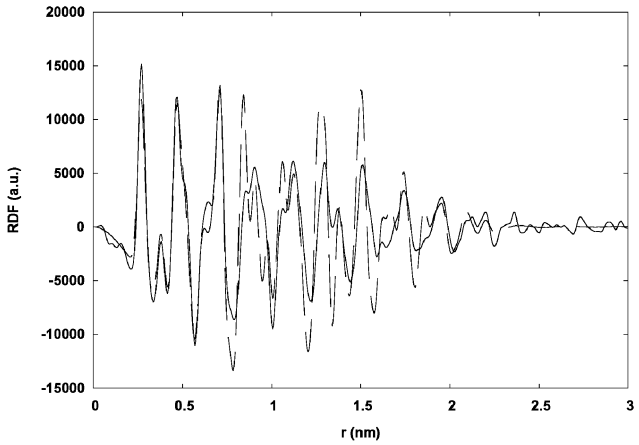


**Fig. 3** Solid line: experimental RDF (radial distribution function) of **Ru1**; dashed line: RDF computed from a spherical model according to bulk ruthenium (1.6 nm in diameter; distances in the model were increased by 1.5% for better agreement with the experimental function).

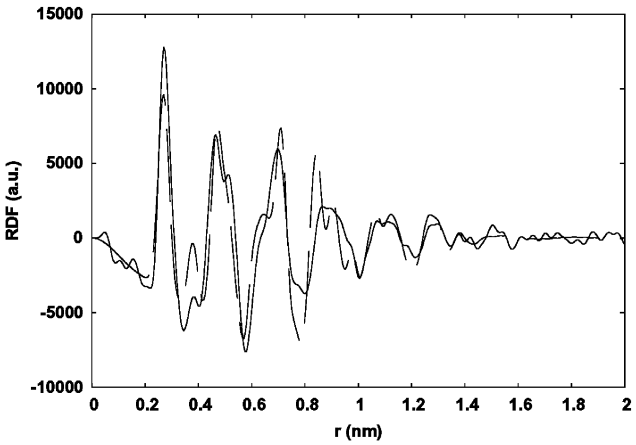


**Fig. 5** Solid line: experimental RDF of **Ru3**; dashed line: RDF computed from a spherical model according to bulk ruthenium (1.6 nm in diameter).

Hydroxy(oxazoline) **4** led to well-dispersed and slightly elongated nanoparticles of 2.7 nm mean size (Fig. 6).

Concerning the bis(oxazoline) ligands, well-defined nanoparticles of very small size (nearly 1.6 nm) and of isotropic shape (**Ru5**–**Ru8**) were obtained in all cases. TEM micrographs of **Ru5** and **Ru6** are shown as representative examples in Fig. 7. These particles are crystalline, as determined by WAXS, with a coherence length close to 1.6 nm, and exhibiting a strong tendency to aggregate into large and regular mesoscopic super-structures.

We have previously noted that platinum nanoparticles stabilized by oxazoline ligands self-assemble into one-dimensional super-structures (''hairs''), due to the formation of hydrogen bond networks, particularly for ligand **4**.[17] Although in the present case, formation of a hydrogen bond network may have occurred, no extended super-structures were observed. Both bis(oxazolines) **5** and **6**, containing, respectively, two and four methylenic groups within their backbone, gave large spherical super-structures (bowls). This organization may result from the coordination of both ends of the ligands to different nanoparticles, in agreement with the very short interparticle distance observed in these objects (*ca.* 1 nm). Such super-structures would then result from the statistical connection between nanoparticles, consistent with the apparent lack of organization in these ''bowls''.

All of these structural observations denote a good argument for the coordination of the ligands used at the surface of the ruthenium particles.

IR spectra were recorded for all samples. However, due to the low overall content in the ligand, the bands displayed a weak intensity (recording more than 100 scans) and consequently, we were unable to reach any structural conclusions.

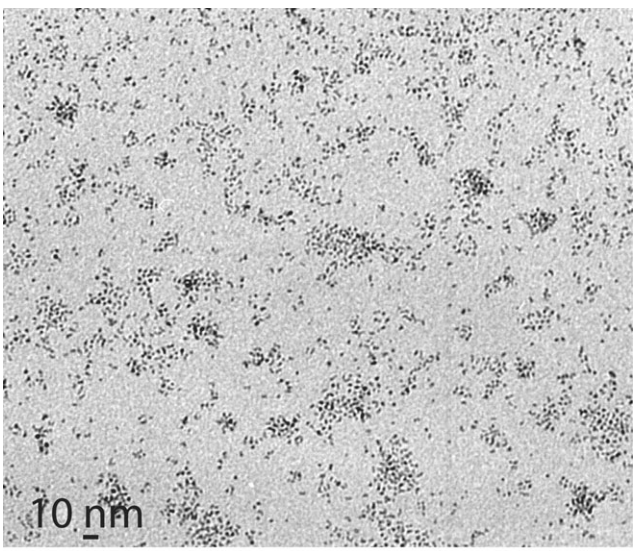


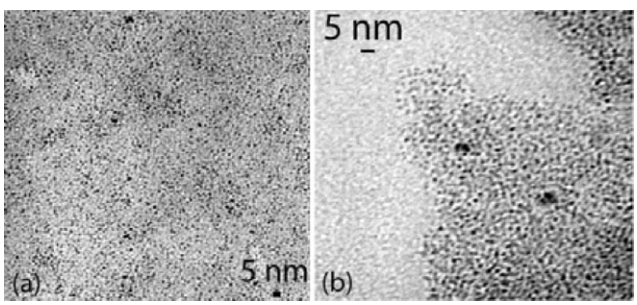


**Fig. 4** TEM micrographs of **Ru2** (a) and **Ru3** (b).

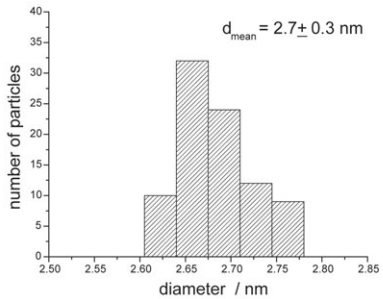


**Fig. 6** TEM micrograph and size histogram of **Ru4**.

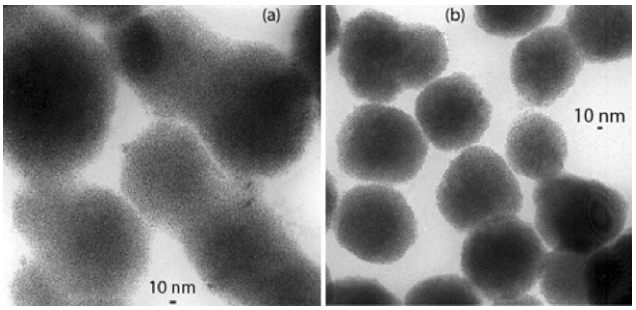


**Fig. 7** TEM micrographs of **Ru5** (a) and **Ru6** (b).



The same held true for our attempts to characterize colloids by $^{1}H$ or $^{13}C$ NMR spectroscopy. In the case of **Ru3**, broad bands by $^{1}H$ NMR were observed, which may be attributable to the equilibrium found at the particle surface between free and coordinated ligand molecules, characteristic of the Ru–hexadecylamine system.[8] In this instance, some dihydrogen, released in the solution, was detected, which was similarly observed for ruthenium colloids stabilized with heptanol[18] or hexadecylamine (HDA).[8] The release of dihydrogen suggests that nanoparticles may additionally contain mobile hydrides at their surface.

## Catalytic reactivity

To demonstrate the coordination chemistry found at the surface of these particles, we decided to evaluate the catalytic reactivity of these new ruthenium colloids. In this way, the selective metal-catalyzed processes offer us a useful tool. An intrinsic problem in the application of colloids as catalysts is the necessity to distinguish between a true colloidal and a molecular catalyst. We therefore chose reactions well-known to be catalyzed by ruthenium complexes, namely, asymmetric hydrogen transfer and hydrogenation.

We will first discuss the results obtained for the asymmetric hydrogen transfer of acetophenone (**I**), using isopropanol as a hydrogen source under basic conditions, and the ruthenium colloids **Ru1**–**Ru8** as catalysts (Table 1). The reactions were carried out at room temperature and monitored by gas chromatography (Scheme 2). The substrate–metal ratio was 20 : 1, whereby the ruthenium amount accounts for all metal atoms included in the nanoparticles (based on the organometallic precursor, [Ru(cod)(cot)]).

When no further free ligand was added in the catalytic medium (entries 1–8, Table 1), the systems were not selective (except **Ru3** which afforded 10% (*S*) for **II**), but did exhibit moderate to high activities (up to 98% conversion after 12 hours, entry 8, Table 1). While certain tests were conducted at low temperature (273 K), enantioselectivity did not improve. Optimum activities corresponded with those ruthenium systems stabilized by amino alcohol **1** (entry 1), amino(oxazoline) **3** (entry 3) and bis(oxazoline) **8** (entry 8). In order to observe the influence of ligand concentration, supplemental free ligand was added to the catalytic medium for the more active systems, **Ru1**, **Ru3**, and **Ru8** (entries 9–14, Table 1). In the three catalytic systems, a remarkable decrease in activity was observed when 1 or 2 equivalents of free ligand (relative to ruthenium) were added (entry 1 *vs.* 9 and 10; entry 3 *vs.* 11 and 12; entry 8 *vs.* 13 and 14), in contrast to the behaviour of the molecular ruthenium catalysts.[12,19] This decrease was even more significant when larger amounts of ligand were added (entry 9 *vs.* 10; entry 13 *vs.* 14). In only the enantioselective system **Ru3**, the total ligand amount in the catalytic medium did not induce changes in the enantiomeric excess of **II** (entries 3, 11 and 12, Table 1).

**Table 1** Ru colloid-catalyzed hydrogen transfer of acetophenone by chiral N-donor ligands (Scheme 2)[a]

| Entry | RuL* | Ru : L*$_{total}$[b] | Time (h) | Conversion (%)[c] | Ee **II** (%)[c] |
|---|---|---|---|---|---|
| 1 | **Ru1** | 1 : 0.2 | 12 | 77 | 0 |
| 2 | **Ru2** | 1 : 0.2 | 12 | 58 | 0 |
| 3 | **Ru3** | 1 : 0.2 | 12 | 65 | 10 (*S*) |
| 4 | **Ru4** | 1 : 0.2 | 12 | 39 | 0 |
| 5 | **Ru5** | 1 : 0.2 | 72 | 14 | 0 |
| 6 | **Ru6** | 1 : 0.2 | 12 | 53 | 0 |
| 7 | **Ru7** | 1 : 0.2 | 48 | 12 | 0 |
| 8 | **Ru8** | 1 : 0.2 | 12 | 98 | 0 |
| 9 | **Ru1** | 1 : 1.2 | 12 | 31 | 0 |
| 10 | **Ru1** | 1 : 2.2 | 12 | 5 | — |
| 11 | **Ru3** | 1 : 1.2 | 12 | 15 | 10 (*S*) |
| 12 | **Ru3** | 1 : 2.2 | 72 | 20 | 10 (*S*) |
| 13 | **Ru8** | 1 : 1.2 | 12 | 79 | — |
| 14 | **Ru8** | 1 : 2.2 | 12 | 56 | — |

[a] 0.12 mmol acetophenone and 0.024 mmol *t*-BuOK in 4 mL of isopropanol, and $6 \times 10^{-3}$ mmol colloid. Results from duplicated experiments. [b] Ruthenium–ligand ratio taking into account the total amount of ligand present in the reaction, from the synthesis of colloid with the extra ligand added to the catalytic reaction. [c] Substrate conversion and ee determined by GC using a chiral column.

Analyzing the catalytic behaviour of these Ru colloids, based on the nature of the ligand, we found that those colloids containing amino functional groups (ligands **1–3**) were more active than hydroxy(oxazoline) (**4**) and bis(oxazolines) (**5–8**). This trend agrees with results published in the literature on molecular Ru catalysts, for which at least one primary or secondary amine moiety must be present in the ligand in order to obtain high yields.[20] For bis(oxazoline) systems (entries 5–8, Table 1), an important backbone effect was observed: those bis(oxazolines) containing shorter spacers (**5** and **7**) were less active than those with longer ones (**6** and **8**), **Ru8** proving to be the most active colloidal catalytic system. Ligands **5**, **6**, and **8** induced the formation of super-structures, probably by using their two oxazoline rings to link to different nanoparticles, and in the case of **8**, to thioether moieties. In contrast, ligands **5** and **7** may have been too firmly fixed on their respective nanoparticles, rendering any approach by the reactants to the metallic surface difficult.

In order to compare the catalytic behaviour between molecular and colloidal ruthenium species, the data corresponding

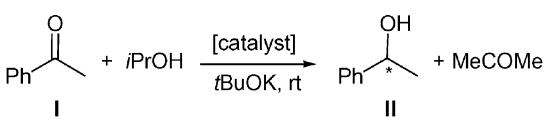


**Scheme 2** Hydrogen transfer of acetophenone catalyzed by ruthenium systems containing N-donor chiral ligands (**L*** = **1–8**).

 

**Table 2** Ru colloids, **RuL***, and the related molecular species, **RuML***, for **L*** = **1–8**, as catalysts in the hydrogen transfer of acetophenone (Scheme 2)[a]

| Entry | L* | Catalyst | Ru : L*$_{total}$[b] | Time (h) | Conversion (%)[c] | Ee **II** (%)[c] |
|---|---|---|---|---|---|---|
| 1 | **1** | **Ru1** | 1 : 0.2 | 12 | 77 | 0 |
| 2 | **1** | **RuM1** | 1 : 1 | 1.5 | 93 | 12 (*R*) |
| 3 | **2** | **Ru2** | 1 : 0.2 | 12 | 58 | 0 |
| 4 | **2** | **RuM2** | 1 : 1 | 12 | 15 | 43 (*R*) |
| 5 | **3** | **Ru3** | 1 : 0.2 | 12 | 65 | 10 (*S*) |
| 6 | **3** | **RuM3** | 1 : 1 | 12 | 55 | 45 (*S*) |
| 7 | **4** | **Ru4** | 1 : 0.2 | 12 | 39 | 0 |
| 8 | **4** | **RuM4** | 1 : 1 | 72 | 0 | 0 |
| 9 | **5** | **Ru5** | 1 : 0.2 | 72 | 14 | 0 |
| 10 | **5** | **RuM5** | 1 : 1 | 20 | 88 | 25 (*S*) |
| 11 | **6** | **Ru6** | 1 : 0.2 | 12 | 53 | 0 |
| 12 | **6** | **RuM6** | 1 : 1 | 12 | 90 | 11 (*R*) |
| 13 | **7** | **Ru7** | 1 : 0.2 | 48 | 12 | 0 |
| 14 | **7** | **RuM7** | 1 : 1 | 20 | 42 | 29 (*S*) |
| 15 | **8** | **Ru8** | 1 : 0.2 | 12 | 98 | 0 |
| 16 | **8** | **RuM8** | 1 : 1 | 12 | 62 | 0 |

[a] 0.12 mmol acetophenone and 0.024 mmol *t*-BuOK in 4 mL of isopropanol; $3 \times 10^{-3}$ mmol $[Ru(p\text{-cymene})Cl_2]_2$ with $6 \times 10^{-3}$ mmol **L*** for molecular catalysts generated *in situ*, **RuML***; or $6 \times 10^{-3}$ mmol of colloid catalyst, **RuL***. Results from duplicated experiments. [b] Ruthenium–ligand ratio, taking into account the total amount of ligand present in the reaction. [c] Substrate conversion and ee determined by GC using a chiral column.

to the molecular systems (**RuM1–RuM8**)[12] and the nanoclusters (**Ru1**–**Ru8**), which are stabilized by the same kind of ligands, were collected in Table 2. We observed that for amino alcohol **1** (entries 1 and 2, Table 2) and bis(oxazolines) **5–7** (entries 9–14, Table 2), the colloidal systems were less active than their corresponding molecular ones. This trend changed, however, for amino(oxazolines) **2** and **3**, as well as for the thioether bis(oxazoline) **8** (entries 3–6 and 15–16, Table 2).

In addition, the **RuM4** molecular system was inactive, while the corresponding colloidal one was active (entry 8 *vs.* 7, Table 2). This suggests a reaction of the molecular precursor resulting from the presence of the phenoxo group (formation of a σ- or π-bonded phenoxide complex), which would render the molecular system inactive, an outcome not seen in ruthenium nanoclusters.[21]

It is also noteworthy that **Ru8** is the fastest colloidal catalyst, even more so than its molecular counterpart (entry 15 *vs.* 16, Table 2). This ligand is quite bulky and contains an aromatic biphenyl backbone capable of interacting with the nanoparticle surface and thioether substituents, which are good electron releasing groups.

The activity behaviour of these systems indicates a specific coordination chemistry of ligands at the metallic surface, depending on the nature of the ligand.

With regard to the selectivity, only the colloidal system stabilized by amino(oxazoline) **3** gives asymmetric induction, lower than that of its corresponding molecular system (entry 5 *vs.* 6, Table 2).

In addition, TEM analysis performed before and after catalysis revealed that the size of ruthenium particles remained unchanged, although some agglomeration was visible.

We also analyzed the behaviour of the sole enantioselective colloidal catalyst, **Ru3**, for the hydrogen transfer reaction, in

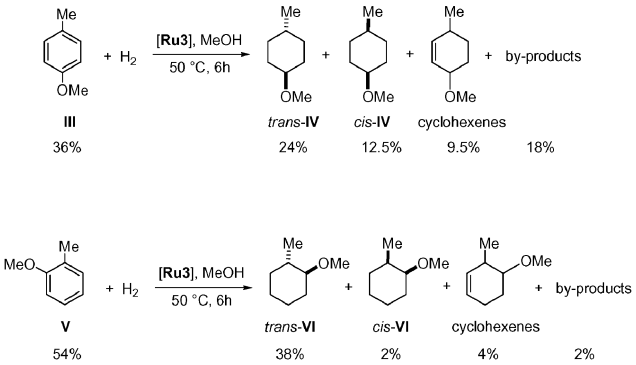


**Scheme 3** Hydrogenation of *ortho*- and *para*-methylanisole catalyzed by the **Ru3** colloidal system [relative percentage following catalysis (determined by GC) is indicated below each chemical].

the hydrogenation of prochiral olefins such as anisole derivatives (**III** and **V**) and dimethyl itaconate (**VII**).

Concerning the disubstituted arenes, *ortho*- and *para*-methylanisole, the molecular system, generated *in situ* from [Ru(cod)(cot)] and ligand **3** (see Experimental section for details), was not found active, in agreement with the well-known trend for catalytic homogenous systems in the reduction of arenes.[3,22] However, under the same conditions (40 bar hydrogen pressure and 50 °C for 6 h), the colloidal system **Ru3** led to a more than 50% conversion of the substrate, with the cyclohexane derivatives (**IV** and **VI**) being the main products: 57% for substrate **III** and 87% for **V** (percentages based on the total amount of detected products). In both cases, the *trans*-isomer was favoured, up to a *trans* : *cis* ratio of 19 : 1 for **VI** (Scheme 3),[23] in contrast to the heterogeneous catalytic systems which favour the *cis*-derivatives.[24] It is important to emphasize that the addition of free ligand (Ru : **3** ratio up to 1 : 0.5) rendered the system completely inactive.

With regard to dimethyl itaconate, **Ru3**, as well as the homogenous analogous system **RuM3**, were found to be active for the hydrogenation of **VII** (Scheme 4). In this particular

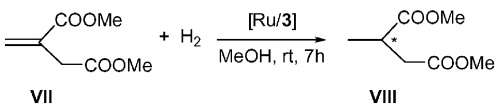


**Scheme 4** Hydrogenation of dimethyl itaconate catalyzed by ruthenium systems containing ligand **3**.

**Table 3** Ru systems containing ligand **3** (colloidal, **Ru3** and molecular, **RuM3**) as catalysts in the hydrogenation of dimethyl itaconate[a]

| Entry | Catalyst | Ru : L*$_{total}$[b] | Conversion (%)[c] | Ee **VIII** (%)[c] |
|---|---|---|---|---|
| 1 | **RuM3** | 1 : 2 | 100 | 18 (*R*) |
| 2 | **Ru3** | 1 : 0.2 | 100 | 0 |
| 3 | **Ru3** | 1 : 0.4 | 80 | 0 |

[a] 2 mmol dimethyl itaconate, 2 mL *n*-butanol (internal standard) and 0.024 mmol *t*-BuOK in 6 mL of methanol; $2 \times 10^{-2}$ mmol **Ru3** or $2 \times 10^{-2}$ mmol [Ru(cod)(cot)] and $4 \times 10^{-2}$ mmol of **3** for molecular catalyst generated *in situ*, **RuM3**. Results from duplicated experiments. [b] Ruthenium–ligand ratio, taking into account the total amount of ligand present in the reaction. [c] Substrate conversion and ee determined by GC using a chiral column.

case, reactions were carried out at room temperature under 40 bar $H_2$ pressure for 7 hours, using a substrate–metal ratio of 100 : 1 (Table 3). When the catalyst was *in situ* generated from [Ru(cod)(cot)] and the free ligand **3** (Ru : **L*** ratio = 1 : 2), total conversion was achieved, giving a low ee, 18% (*R*) for product **VIII** (entry 1, Table 3). When a colloidal catalyst was used, activity was also high, but without inducing any enantiomeric excess (entries 2 and 3, Table 3). Analogous with the behaviour observed in acetophenone hydrogen transfer, the addition of free ligand in the catalytic medium effected a decrease in activity (entry 2 *vs.* 3, Table 3).

## Conclusions

Ruthenium nanoparticles stabilized by chiral ligands were prepared in an easy and reproducible way. Depending on the stabilizer employed, different shapes and sizes were observed.

Surface coordination of ligands not only led to an excellent stabilization of metal particles in solution, but also strongly influenced their catalytic behaviour. Mean diameters *ca.* 2.5 nm were found using mono(oxazoline) ligands, and *ca.* 1.6 nm with bis(oxazolines). These trends are consistent with the size decrease observed when ligand concentration increases, as well as with the coordinating behaviour of bis(oxazolines), chelate and bridge effects.

One of the goals of this study was to find evidences for differentiating colloidal from molecular catalysts. In the present work, four clues agree with this objective. First, ligand **5** poisons the molecular system, probably through formation of a Π-bonded phenoxo complex, which was not observed in the colloids. Second, ligand **8**, which offers multiple possibilities for interaction with the colloidal surface (nitrogen, sulfur, Π-system), is a better promoter of colloidal than molecular catalysis. Third, in the three studied processes, the addition of excess ligand decreased the activity of the catalytic system without any effect on the selectivity; whereas an increase of ee would be expected in the case of metal leaching to form a molecular catalyst. And fourth, the ruthenium colloidal system stabilized by ligand **3**, was active in the reduction of arene derivatives, in manifest contrast to the analogous mononuclear systems. The very low asymmetric induction encountered when colloidal catalysts are used, compared with molecular systems, suggests a fluxional behaviour of the ligands at the surface of ruthenium nanoparticles, as recently described for Ru–amine colloids.

To conclude, this study demonstrates the need to design appropriate ligands, capable of binding to nanoparticles, as well as of performing target reactions. This may well be the case with ligand **8** which displays several sites of coordination. Future work in this field should include this goal in order to better exploit the adaptability of these colloidal systems.

## Experimental

### General

All operations were carried out using Schlenk tube or Fisher–Porter bottle techniques under argon. $RuCl_3 \cdot H_2O$ (Strem), $[Ru(\eta^6\text{-}p\text{-cymene})Cl(\mu\text{-}Cl)]_2$ (Strem), *t*-BuOK (Fluka), (*R*)-(+)-2-aminobutanol (Fluka) and L-valinol (Aldrich) were purchased and used without prior purification. HPLC grade isopropanol was purchased from Fluka. The other reagents were purchased from Aldrich and most of the solvents from SDS. The solvents were distilled under a nitrogen atmosphere. THF was refluxed over sodium benzophenone, pentane over calcium hydride, and methanol over magnesium after activation with iodine. All reagents and solvents were degassed under vacuum at liquid nitrogen temperature by 3 vacuum–argon cycles.

[Ru(cod)(cot)] was prepared according to a published procedure.[16] It was purified by recrystallization in pentane and the resulting highly sensitive yellow crystals were stored under argon at −30 °C. Their purity was checked by elemental analysis and $^1$H-NMR spectroscopy. Mono- and bis(oxazoline) ligands were prepared as previously described.[12b,13a,13b]

Specimens for TEM analysis were prepared by slow evaporation of a drop of colloidal solution deposited under argon onto holey carbon-covered copper grids. The TEM experiments were performed at the "Service Commun de Microscopie Electronique de l'Université Paul Sabatier" using a JEOL 200 CX-T electron microscope operating at 200 kV and a Philips CM12 electron microscope operating at 120 kV, with respective point resolutions of 4.5 and 5 Å. HRTEM observations were carried out with a JEOL JEM 2010 electron microscope working at 200 kV with a resolution point of 2.5 Å. Transmission electron microscopy was used as a standard tool of analysis for determining the mean size of ruthenium particles. Size distribution of the particles was determined by manual analysis of enlarged images by measuring at least 200 particles on a given grid to obtain a statistical size distribution as well as a mean diameter.

Data collection for the wide-angle X-ray scattering was performed on small amounts of powder at the CEMES/CNRS, Toulouse.

NMR spectra of particles were recorded on Bruker DRX 250 or 400 MHz (standard $SiMe_4$) spectrometers, using THF-$d_8$ as solvent. Chemical shifts were reported downfield from standards. IR spectra were recorded on a Perkin Elmer spectrometer GX (FT-IR system). Colloid samples were prepared as KBr pellets, unless otherwise stated.

Elemental analyses were performed in the "Services d'Analyses du CNRS" at the LCC in Toulouse for carbon, nitrogen and hydrogen determinations, and at the "Service Central d'Analyse" in Lyon for ruthenium, sulfur and oxygen determinations.

GC analyses were performed on a Hewlett-Packard 5890 Series II gas chromatograph (50 m Ultra 2 capillary column) with an FID detector. Enantiomeric excesses were determined by GC on FS-cyclodex-β-I/P and FS-cyclodex-α-I/P columns.

### General synthesis of Ru particles stabilized by asymmetric organic ligands

In a typical experiment, 150 mg of [Ru(cod)(cot)] (0.476 mmol) was introduced in a Fisher–Porter bottle and left in a vacuum for 30 minutes. 125 mL of solvent (neat THF or THF–methanol mixture), degassed by freeze–pump cycles, was then

 

added. The resulting yellow solution was cooled to 193 K after which a 25 mL solution of THF containing 0.2 equivalents of the ligand was placed in the flask. The bottle was pressurized under 3 bar of dihydrogen and the solution allowed to slowly warm to room temperature under vigorous stirring. After 24 hours a homogenous brown solution was obtained. After elimination of excess dihydrogen, approximately 3 mL of the solution was passed under argon over a small alumina column. The absence of filtrate colour indicated full decomposition of the precursor. The volume of the solution was then reduced to approximately 15 mL. 50 mL of deoxygenated pentane was then added and the resulting mixture cooled to 193 K at which temperature a brown precipitate formed after several hours. Following filtration, the precipitate was washed with pentane ($2 \times 50$ mL of deoxygenated pentane) and dried under reduced pressure. The resulting particles were obtained as dark brown powders. In all cases, ruthenium colloids were found to remain stable over time and did not exhibit any signs of decomposition. They were characterized by IR spectroscopy, TEM, and WAXS analysis.

**Ru1.** Solvent used in the synthesis: THF. IR ($cm^{-1}$): 3431, 2959, 2915, 2846, 1926, 1627. Elemental analysis (%): Ru = 48.9, C = 7.6, H = 4.1, N = 1.3, O = 1.2. Mean diameter (TEM, nm) = 2.5.

**Ru2.** Solvent used in the synthesis: THF. IR ($cm^{-1}$): 3392, 2963, 2927, 2877, 1610. Elemental analysis (%): Ru = 49.3, C = 12.7, H = 6.1, N = 1.1, O = 0.9. Mean diameter (TEM, nm) = 2.5.

**Ru3.** Solvent used in the synthesis: THF. IR ($cm^{-1}$): 3409, 2959, 2922, 2856, 1610. Elemental analysis (%): Ru = 49.6, C = 12.1, H = 5.3, N = 1.2, O = 1.3. Mean diameter (TEM, nm) = 2.0.

**Ru4.** Solvent used in the synthesis: THF. IR ($cm^{-1}$): 3411, 2950, 2921, 2858, 1606. Elemental analysis (%): Ru = 46.1, C = 13.2, H = 6.1, N = 0.3, O = 2.3. Mean diameter (TEM, nm) = 2.7.

**Ru5.** Solvent used in the synthesis: THF. IR ($cm^{-1}$): 2907, 2841, 1638. Elemental analysis (%): Ru = 44.2, C = 12.7, H = 5.3, N = 0.9, O = 1.8. Mean diameter (TEM, nm) = 1.6.

**Ru6.** Solvent used in the synthesis: THF–MeOH. IR ($cm^{-1}$): 2900, 2844, 1623. Elemental analysis (%): Ru = 44.3, C = 16.4, H = 0.9, N = 0.7, O = 0.9. Mean diameter (TEM, nm) = 1.5.

**Ru7.** Solvent used in the synthesis: THF. IR ($cm^{-1}$): 3411, 2950, 2921, 2858, 1606. Elemental analysis (%): Ru = 45.0, C = 14.2, H = 7.1, N = 0.8, O = 1.7. Mean diameter (TEM, nm) = 1.6.

**Ru8.** Solvent used in the synthesis: THF–MeOH. IR ($cm^{-1}$): 3407, 2907, 2841, 1627. Elemental analysis (%): Ru = 47.1, C = 16.1, H = 9.2, N = 0.8, O = 0.8, S = 0.9. Mean diameter (TEM, nm) = 1.6.

### Catalytic reactions

Blank tests were carried out in order to evaluate the stability of the ligands under the catalytic conditions. No hydrogenation reactions were detected in any case.

**Asymmetric hydrogen transfer of acetophenone.** 0.12 mmol of acetophenone (2 mL of solution 0.06 M in isopropanol) and 0.024 mmol of *t*-BuOK (2 mL of solution 0.012 M in isopropanol) were mixed at room temperature. $6 \times 10^{-3}$ mmol of colloid catalyst **RuL** (based on starting [Ru(cod)(cot)] complex) in the presence of varying amounts of ligand **L*** (0.2, 1.0 or 2.0 equivalents, relative to the ruthenium; for molecular catalysts generated *in situ*: $3 \times 10^{-3}$ mmol $[Ru(p\text{-cymene})Cl_2]_2$ with $6 \times 10^{-3}$ mmol **L***) were then added. The reactions were monitored by GC. Enantiomeric excesses and conversions were determined by GC on a chiral column.

**Asymmetric hydrogenation of dimethyl itaconate.** 2 mmol of dimethyl itaconate, 2 mL *n*-butanol and $2 \times 10^{-2}$ mmol of **Ru3** (for the molecular catalysts generated *in situ*: $2 \times 10^{-2}$ mmol of [Ru(cod)(cot)] with $4 \times 10^{-2}$ mmol of **3**) were dissolved in 6 mL of methanol at room temperature in an autoclave. Molecular hydrogen was then introduced until 40 bar of pressure was attained. The reaction was stirred for 7 h. The solution was filtered over celite and purified by column chromatography ($SiO_2$; ethyl acetate). Enantiomeric excesses and conversions were determined by GC on a chiral column.

**Asymmetric hydrogenation of *para*- and *ortho*-methylanisole.** 6 mmol of methylanisole (724.4 mg) and $6 \times 10^{-2}$ mmol of **Ru3** (6 mg, based on [Ru(cod)(cot)]) were dissolved in 10 mL of methanol at 50 °C in an autoclave (for the molecular catalysts generated *in situ*: $2 \times 10^{-2}$ mmol of [Ru(cod)(cot)] with $4 \times 10^{-2}$ mmol of **3**). Molecular hydrogen was then introduced until 40 bar of pressure was attained. The reaction was stirred for 6 h. The solution was filtered over celite and the solution analyzed by GC. Catalyses were also carried out in the presence of free ligand, using a mixture of $6 \times 10^{-2}$ mmol of **Ru3** and $6 \times 10^{-3}$ mmol of **3** as a catalytic precursor.

## Acknowledgements

The authors are very grateful to V. Collière for his contribution to TEM/HRTEM analysis and the TEMSCAN (Service Commun de Microscopie Electronique de l'Université Paul Sabatier). We would also like to thank CNRS, Egide (PAI Picasso No 04230PL), the *Ministerio de Educación y Ciencia* (CTQ2004-01546/BQU; *Acción integrada* HF2001-0024) and the *Generalitat de Catalunya* for financial support. M. G. would like to thank the *Ministerio de Educación, Cultura y Deporte* (PR2000-0178 0077107784) for a sabbatical grant.

## References

1 (*a*) K. J. Klabunde and G. Cardenas-Trivano, in *Active Metals Preparation, Characterization, Applications*, ed. A. Fürstner, VCH, Weinheim, 1996, p. 237; (*b*) *Nanoparticles from theory to applications*, ed. G. Schmid, VCH, Weinheim, 2004.
2 (*a*) G. Schmid, *Chem. Rev.*, 1992, **92**, 1709; (*b*) L. N. Lewis, *Chem. Rev.*, 1993, **93**, 2693; (*c*) D. Aiken III and R. G. Finke, *J. Mol. Catal. A: Chem.*, 1999, **145**, 1; (*d*) M. A El-Sayed, *Acc. Chem. Res.*,

2001, **34**, 257; (*e*) H. Bönnemann and R. M. Richards, *Eur. J. Inorg. Chem.*, 2001, 2455.
3 A. Roucoux, J. Schulz and H. Patin, *Chem. Rev.*, 2002, **102**, 3757.
4 J. A. Widegren and R. G. Finke, *J. Mol. Catal. A: Chem.*, 2003, **191**, 187.
5 (*a*) I. W. Davies, L. Matty, D. L. Hughes and P. J. Reider, *J. Am. Chem. Soc.*, 2001, **123**, 10139; (*b*) J. A. Widegren and R. G. Finke, *J. Mol. Catal. A: Chem.*, 2003, **191**, 317.
6 K. Philippot and B. Chaudret, *C. R. Chim.*, 2003, **6**, 1019.
7 C. Pan, K. Pelzer, K. Philippot, B. Chaudret, F. Dassenoy, P. Lecante and M.-J. Casanove, *J. Am. Chem. Soc.*, 2001, **123**, 7584.
8 T. Pery, K. Pelzer, J. Mathes, G. Buntkowski, K. Philippot, H.-H. Limbach and B. Chaudret, *ChemPhysChem*, 2005, **6**, 605.
9 (*a*) M. Studer, H.-U. Blaser and C. Exner, *Adv. Synth. Catal.*, 2003, **345**, 45; (*b*) H. Bönnemann and G. A. Braun, *Angew. Chem., Int. Ed. Engl.*, 1996, **35**, 1992; (*c*) H. Bönnemann and G. A. Braun, *Chem.–Eur. J.*, 1997, **3**, 1200; (*d*) X. Zuo, H. Liu, D. Guo and X. Yang, *Tetrahedron*, 1999, **55**, 7787; (*e*) J. U. Köhler and J. S. Bradley, *Catal. Lett.*, 1997, **45**, 203; (*f*) J. U. Köhler and J. S. Bradley, *Langmuir*, 1998, **14**, 2730; (*g*) M. Tamura and H. Fujihara, *J. Am. Chem. Soc.*, 2003, **125**, 15742; (*h*) V. Mévellec, C. Mattioda, J. Schulz, J.-P. Rolland and A. Roucoux, *J. Catal.*, 2004, 1.
10 V. Mévellec, A. Roucoux, E. Ramirez, K. Philippot and B. Chaudret, *Adv. Synth. Catal.*, 2004, **346**, 72.
11 S. Jansat, M. Gómez, K. Philippot, G. Muller, E. Guiu, C. Claver, S. Castillón and B. Chaudret, *J. Am. Chem. Soc.*, 2004, **126**, 1592.
12 (*a*) M. Gómez, S. Jansat, G. Muller, M. C. Bonnet, J. A. J. Breuzard and M. Lemaire, *J. Organomet. Chem.*, 2002, **659**, 186; (*b*) M. Gómez, S. Jansat, G. Muller, S. Alvarrez, G. Aullón and M. A. Maestro, *Eur. J. Inorg. Chem.*, 2005, 4341.
13 (*a*) M. Gómez, S. Jansat, G. Muller, M. A. Maestro, J. Mahía, M. Font-Bardía and X. Solans, *J. Chem. Soc., Dalton Trans.*, 2001, 1432; (*b*) M. Gómez, S. Jansat, G. Muller, M. A. Maestro and J. Mahía, *Organometallics*, 2002, **21**, 1077; (*c*) M. A. Pericàs, C. Puigjaner, A. Riera, A. Vidal-Ferran, M. Gómez, F. Jiménez, G. Muller and M. Rocamora, *Chem.–Eur. J.*, 2002, **8**, 4164; (*d*) D. Franco, M. Gómez, F. Jiménez, G. Muller, M. Rocamora, M. A. Maestro and J. Mahía, *Organometallics*, 2004, **23**, 3197.
14 (*a*) J. A. Brito, M. Gómez, G. Muller, H. Teruel, J. C. Clinet, E. Duñach and M. A. Maestro, *Eur. J. Inorg. Chem.*, 2004, 4278; (*b*) M. Gómez, S. Jansat, G. Muller, G. Noguera, H. Teruel, V. Moliner, E. Cerrada and M. Hursthouse, *Eur. J. Inorg. Chem.*, 2001, 1071.
15 M. Henning, K. Püntener and M. Scalone, *Tetrahedron: Asymmetry*, 2000, **11**, 1849.
16 P. Pertici and G. Vitulli, *Inorg. Synth.*, 1983, **22**, 17.
17 M. Gómez, K. Philippot, V. Collière, P. Lecante, G. Muller and B. Chaudret, *New J. Chem.*, 2003, **27**, 114.
18 K. Pelzer, K. Philippot and B. Chaudret, *Z. Phys. Chem.*, 2003, **217**, 1539.
19 D. G. I. Petra, P. C. J. Kamer, P. W. N. M. van Leeuwen, K. Goubitz, A. M. van Loon, J. G. de Vries and H. E. Schoemaker, *Eur. J. Inorg. Chem.*, 1999, 2335.
20 R. Noyori and S. Hashiguchi, *Acc. Chem. Res.*, 1997, **30**, 97.
21 D. J. Cole-Hamilton, R. J. Young and G. Wilkinson, *J. Chem. Soc., Dalton Trans.*, 197619), 1995.
22 G. Süss-Fink, M. Faure and T. R. Ward, *Angew. Chem., Int. Ed.*, 2002, **41**, 99.
23 GC (with α- and β-cyclodextrin columns) and HPLC (with an OD chiral column) analyses were carried out under several conditions, without achieving separation of enantiomers.
24 A. Roucoux, J. Schulz and H. Patin, *Adv. Synth. Catal.*, 2003, **345**, 222.



 